Article type: Research Article

Received May 28, 2024; Accepted May 28, 2024

Edited by xxxx

Running title: Biosynthesis of natural statin melitidin

Overexpression of Tonoplast Ca^{2+}-ATPase in Guard Cells Synergistically Enhances Stomatal Opening and Drought Tolerance

Jinghan Su[1†], Bingqing He[1†], Peiyuan Li[1], Baiyang Yu[1], Qiwen Cen[1], Lingfeng Xia[2], Yi Jing[3], Feibo Wu[1], Rucha Karnik[2], Dawei Xue[4], Michael R. Blatt[2] and Yizhou Wang[1,5*]

[1]Institute of Crop Science, Zhejiang University, Hangzhou 310058, China.

[2]Laboratory of Plant Physiology and Biophysics, University of Glasgow, Glasgow G12 8QQ, UK.

[3]BGI Research, Sanya 572025, China

[4]College of Life and Environmental Sciences, Hangzhou Normal University, Hangzhou 311121, China

[5]Zhejiang Provincial Key Laboratory of Crop Germplasm, Zhejiang University, Hangzhou 310058, China

[†]These authors contributed equally to this work

[*]Corresponding authors: Yizhou Wang (Email: wangyizhou@zju.edu.cn; Tel: 0571-88982585)

ORCIDS

Jinghan Su: 0009-0004-2617-5316

Bingqing He: 0009-0000-2908-1762

Peiyuan Li: 0009-0005-2242-6445

Baiyang Yu: 0009-0003-1209-7946

Qiwen Cen: 0000-0001-8768-0114

Lingfeng Xia: 0000-0002-8628-8062

Yi Jing:

Feibo Wu: 0000-0001-8797-3398

Rucha Karnik: 0000-0001-6876-4099
Dawei Xue: 0000-0001-9904-7615
Michael R. Blatt: 0000-0003-1361-4645
Yizhou Wang: 0000-0002-2188-383X

ABSTRACT Stomata play a crucial role in plants by controlling water status and responding to drought stress. However, simultaneously improving stomatal opening and drought tolerance has proven to be a significant challenge. To address this issue, we employed the OnGuard quantitative model, which accurately represents the mechanics and coordination of ion transporters in guard cells. With the guidance of OnGuard, we successfully engineered plants that overexpress the main tonoplast Ca^{2+}-ATPase gene, *ACA11*, which promotes stomatal opening and enhances plant growth. Surprisingly, these transgenic plants also exhibited improved drought tolerance due to reduced water loss through their stomata. Again, OnGuard assisted us in understanding the mechanism behind the unexpected stomatal behaviours observed in the *ACA11* overexpressing plants. Our study reveals that the overexpression of *ACA11* facilitates the accumulation of Ca^{2+} in the vacuole, thereby influencing Ca^{2+} storage and leading to an enhanced Ca^{2+} elevation in response to ABA. This regulatory cascade finely tunes stomatal responses, ultimately leading to enhanced drought tolerance. Our findings underscore the importance of tonoplast Ca^{2+}-ATPase in manipulating stomatal behaviour and improving drought tolerance. Furthermore, these results highlight the diverse functions of tonoplast-localized ACA11 in response to different conditions, emphasizing its potential for future applications in plant enhancement
Keywords: Stomata, Guard Cells, ACA11, Modelling, Drought

INTRODUCTION

Stomata are vital for maintaining water status and responding to drought stress in plants. These small pores, primarily located on the surface of leaves, control the exchange of gases and water vapour (Hetherington and Woodward, 2003; Wang et al., 2022). Under normal conditions, stomata open to allow the entry of carbon dioxide (CO_2) required

for photosynthesis. However, in the face of drought, plants confront the challenge of water scarcity and the need to prevent excessive water loss through transpiration (Lawson et al., 2011; Gupta et al., 2020). As a result, plants employ various mechanisms to adjust the stomatal aperture, striking a balance between CO_2 capture and water conservation. Unfortunately, these adjustments result in stomatal closure, which diminishes the uptake of CO_2 for photosynthesis and consequently hampers plant growth (Lawson and Blatt, 2014; Blatt et al., 2017; Lawson and Vialet-Chabrand, 2019). Consequently, the intrinsic relation between stomatal aperture and drought tolerance creates a significant barrier when it comes to simultaneously improving stomatal function and drought tolerance.

Guard cells play an important role in regulating the opening and closing of stomata. This regulation occurs through changes in osmotic solute uptake and loss, particularly K^+ and Cl^-, as well as the synthesis and metabolism of organic solutes that drive water movement through the guard cells (Kim et al., 2010; Jezek and Blatt, 2017; Wang et al., 2018). Under drought stress, ABA triggers an elevated concentration of free cytosolic calcium ($[Ca^{2+}]_i$) plays a pivotal role in regulating the transport of ions across the guard cell membrane (Kim et al., 2010; Lee and Luan, 2012; Munemasa et al., 2015). This leads to the efflux of K^+ and anions, causing a net loss of osmotic content, which in turn reduces turgor pressure and volume within the guard cells, ultimately resulting in the closure of stomatal pores (Blatt, 2000; Wang et al., 2018). These studies raise an intriguing question: is it possible to manipulate the ion transport processes in guard cells in order to enhance stomatal opening and promote plant growth under normal conditions, while still allowing them to promptly close stomata in response to drought stress? Understanding the mechanics and coordination of ion transporters within the guard cells could provide valuable insights into how these processes could be engineered to enhance stomatal opening in synchrony with drought tolerance, thereby enabling plants to survive under water-limited conditions while maintaining efficient gas exchange for photosynthesis.

To address this challenge, we take advantage of the guard cell quantitative model, OnGuard, to explore the *in silico* potential for enhancing stomatal aperture and drought

tolerance. OnGuard is the first quantitative model specifically designed for guard cells and offers a comprehensive set of macroscopic descriptors for their unique characteristics (Chen et al., 2012; Hills et al., 2012; Blatt et al., 2022; Rui et al., 2022). The reliability of the model's representations has been established across a wide range of experiments (Wang et al., 2012; Wang et al., 2017; Jezek et al., 2019; Jezek et al., 2021; Horaruang et al., 2022), providing a deeper understanding of the intricate mechanisms regulating the responses of guard cells and stomata to environmental changes (Wang et al., 2017; Jezek et al., 2021; Horaruang et al., 2022). As a result, the predictive capability of the OnGuard model is crucial in guiding the reverse engineering of stomatal function, starting from *in silico* molecular manipulations (Blatt et al., 2022; Rui et al., 2022).

With the guidance of OnGuard, we have successfully generated transgenic plants that overexpress *ACA11* (Lee et al., 2007; Boursiac et al., 2010), a major tonoplast-localized Ca^{2+}-ATPases, that promotes stomatal opening and enhancing plant growth. Surprisingly, our experiments have revealed that the plants with an overexpressed *ACA11* demonstrate improved drought tolerance due to a reduction in water loss through their stomata. Once again, OnGuard assists in uncovering the mechanism behind the counterintuitive stomatal behaviours observed in the *ACA11* overexpressing plants.

Our finding indicated that overexpressing *ACA11* promotes Ca^{2+} accumulation in the vacuole. Under optimal conditions, this accumulation of Ca^{2+} plays a crucial role in facilitating stomatal opening, which in turn allows for the carbon assimilation and promotes plant growth. However, in response to drought conditions, the elevated levels of Ca^{2+} actually promote stomatal closure, leading to a reduction in water loss and an enhancement of drought tolerance. These findings highlight the importance of employing quantitative modelling techniques to guide the engineering of stomatal behaviour. Furthermore, they demonstrate the potential of tonoplast ACA11 to manipulate stomatal behaviour and improve drought tolerance for future applications in plant enhancement.

RESULTS

In silico analysis of manipulating key membrane transporters to enhance stomatal aperture

We first evaluated the sensitivity of major membrane transporters to variations within a narrow range of genetically tractable parameters. Given that changes in certain transporters have a significant impact on stomatal aperture, we made gentle adjustments to their densities by increasing them two-fold (×2) or decreasing them by half (×0.5) to simplify our simulations (Appendix A1). The other settings used for modelling were consistent with previously described methods (Wang et al., 2014; Wang et al., 2017).

We quantified the model outputs by considering two variables: the maximum aperture (Ap_{max}) and the minimum aperture (Ap_{min}), as shown in Fig. 1A. Fig. 1B provides a summary of the quantitative information for these two values. It is worth noting that most changes in the population of transporters had minimal or no impact on stomatal aperture (Fig. 1B and Table S1). However, through our analysis, we were able to identify several transporters that play a crucial role in enhancing stomatal aperture. By manipulating their population, we are able to achieve larger Ap_{max} and Ap_{min} compared to the wild-type plants (Fig.1C and Table S1). Notably, several manipulations on Ca^{2+} transporters, including ×2 tonoplast Ca^{2+}-ATPase (tACA) and ×0.5 plasma membrane voltage-gated Ca^{2+} channel (VCa), ×0.5 tonoplast voltage-gated Ca^{2+} channel (tVCa) and ×2 plasma membrane Ca^{2+}-ATPase (ACA) were found to have the greatest impact on enhancing both Ap_{max} and Ap_{min} (Fig.1c and Table S1). Considering the limited availability of biological information on VCa and tVCa, we have decided to shift our focus to tACA in our upcoming study. This particular manipulation primarily enhances Ap_{max} when compared to ACA (Fig.1C and Table S1).

Ca^{2+}-ATPases are recognized as key players in maintaining cellular Ca^{2+} levels (Evans and Williams, 1998; Garcia Bossi et al., 2020). In *Arabidopsis*, tonoplast Ca^{2+}-ATPases ACA4 and ACA11 are believed to impact endomembrane Ca^{2+} stores and are associated with (a)biotic stress response (Boursiac et al., 2010; Jezek et al., 2021). *ACA4* is predominantly expressed on pre-vacuoles (Geisler et al., 2000; Boursiac et al.,

2010), and in order to validate the predictions of our model, we generated transgenic plants that overexpressed *ACA11*, the primary Ca^{2+}-ATPase on the tonoplast (Lee et al., 2007; Boursiac et al., 2010). To achieve this, we used a strong promoter that is specific to guard cells to drive the expression of *ACA11* in the wild-type plants, created *GC1::ACA11* and *GC1::ACA11*-GFP lines. The confocal imaging unambiguously displayed the presence of GFP signals originating from the guard cells (Fig. S1). Additionally, quantitative (q) PCR analysis showed that the *ACA11* transcripts in the epidermal tissue of the transgenic plants, which included the guard cells, were approximately 5-fold higher in comparison to the wild-type plants (Fig. S2). Interestingly, in addition to the increased expression of *ACA11*, we also observed elevated expression levels of the inward rectifying K^+ channel genes (*KAT1* and *KAT2* (Pilot et al., 2003)), the outward rectifying K^+ channel gene (*GORK* (Hosy et al., 2003)), and the slow anion channel genes (*SLAC1* and *SLAH3* (Negi et al., 2008; Vahisalu et al., 2008)) (Fig. S2).

Simulating the impact of tonoplast Ca^{2+}-ATPase on stomatal aperture

To investigate the effects of manipulating the expression level of tonoplast Ca^{2+}-ATPase, we employed OnGuard to analyse stomatal aperture and predict the resulting consequences. Initially, our simulations involved the full complement of membrane transporters, referred to as the wild-type. Subsequently, we conducted simulation to evaluate the overexpression of tonoplast Ca^{2+}-ATPase (referred to as *ox tACA*), with transporter population densities adjusted to a 5-fold factor. According to the qPCR results (Fig. S2), we have also increased the population of Kin and Kout by a factor of 2, and SLAC by a factor of 3. Additionally, we have increased tVCa by a factor of 2 to ensure a balanced Ca^{2+} flux across the tonoplast (Appendix A2). Fig.2 provides a summary of the macroscopic outputs derived from the OnGuard modelling. Notably, increasing the population of tonoplast Ca^{2+}-ATPase had significant effects on the dynamic range of stomatal conductance (g_s, Fig. 2A), leading to elevated values for both maximum (Opened) and minimum (Closed) aperture (Fig. 2B). The increase in aperture had a positive effect on photosynthesis (A; Fig. 2C), intercellular CO_2

concentration (C_i; Fig. 2D), and transpirational rate (*E*; Fig. 2E). However, the *ox tACA* mutants exhibits a slightly lower water use efficiency (WUE; Fig. 2F).

Microscopic outputs from OnGuard has demonstrated the impact of overexpressing tonoplast Ca^{2+}-ATPase on the major ion fluxes in guard cells (Fig. 3 and Fig. S3-S6). In general, the overexpression of tonoplast Ca^{2+} transporters promote the influx of Ca^{2+} into the vacuole, resulting in a reduction in $[Ca^{2+}]_i$ (Fig. 3I and Fig. S6). It is well-known that $[Ca^{2+}]_i$ has an influence on the activation of plasma membrane H^+-ATPases (Blatt, 1999, 2000; Jezek and Blatt, 2017; Wang et al., 2018). By lowering $[Ca^{2+}]_i$, the plasma membrane H^+-ATPases are activated (Fig. S5), resulting in the influx of Cl^- through plasma membrane H^+-Cl^- antiporters (Fig. S4) and an increase in the cytosolic Cl^- content (Fig. 3E). Moreover, the reduction in $[Ca^{2+}]_i$ also activates of plasma membrane Kin, in conjunction with the increased Kin population, thereby enhancing the influx of K^+ (Fig. S3) and an elevated K^+ accumulation (Fig. 3C). Consequently, these mechanisms collectively contribute to an increase in osmotic pressure within guard cells, ultimately leading to a larger stomatal aperture in *ox tACA.*

GC1::ACA11 plants exhibit larger stomatal aperture and improved growth

We conducted an analysis on *GC1::ACA11* lines to validate the predictions made by the model. When exposed to 2 hours of light illumination, the *GC1::ACA11* lines exhibited stomatal apertures that were approximately 30% wider compared to the wild-type plants (Fig. 4A and B). Similarly, when kept in darkness, the transgenic plants displayed stomatal apertures that were around 16% wider (Fig. 4A and B). In order to monitor the changes in stomatal movements, we also recorded g_s from intact plants in response to step changes in light. As anticipated, the measurements of gas exchange revealed higher g_s in the *GC1::ACA11* lines compared to the wild-type plants (Fig. 4C). As a result, these findings provide further support for the model's prediction that overexpressing *ACA11* leads to an enlargement of stomatal apertures.

We next conducted a detailed examination of photosynthetic activity in intact leaves of *GC1::ACA11* transgenic plants. Fig. 4D clearly demonstrates that the CO_2 assimilation rate was significantly higher in the *GC1::ACA11* lines compared to the wild-type plants. To determine whether the increased photosynthetic rate in

GC1::ACA11 plants was due to an enlarged stomatal aperture, we analysed the response curve between the CO_2 assimilation rate and the leaf intercellular CO_2 concentration under saturating-light conditions (Fig. 4D). The CO_2 response curves for *GC1::ACA11* lines and wild-type plants were nearly identical, indicating that both the Rubisco carboxylation capacity and the electron transport capacity were similar (Fig. 4D). Thus, the improved photosynthetic efficiency is largely due to the increased g_s. Consequently, after 4 weeks of growth, the *GC1::ACA11* plants displayed a larger rosette area and approximately 45% higher dry weights compared to the wild-type plants (Fig. 4E and F). In contrast, the WUE of *GC1::ACA11* plants was significantly lower than that of wild-type plants (Fig.4E and F). However, it is worth mentioning that the stomatal density of the *GC1::ACA11* plants was comparable to that of the wild-type plants (Table S2).

GC1::ACA11 plants surprisingly exhibits improved drought tolerance

The overexpression of *ACA11* in guard cells has been shown to have contrasting effects on plant physiology. Under favourable conditions, it promotes stomatal aperture and reduces WUE. However, these changes are believed to be disadvantageous for drought tolerance, as they increase water loss during drought conditions. To investigate the long-term effects of *ACA11* overexpression on drought tolerance, we conducted drought experiments using wild-type plants and *GC1::ACA11* lines. Two-week-old plants of both types were subjected to water withholding conditions for 20 days. Surprisingly, when we exposed the plants to drought conditions, we observed that the *GC1::ACA11* lines exhibited enhanced drought tolerance (Fig. 5A). After re-watering, the survival rate of *GC1::ACA11* lines was significantly higher than that of wild-type (Fig. 5A and B).

Contrary to the observations under normal conditions, the *GC1::ACA11* lines exhibited smaller stomatal aperture under drought conditions (Fig. 5C). To further investigate this phenomenon, we employed infrared thermography to analyse these plants. Under normal conditions, the *GC1::ACA11* lines exhibited lower leaf temperatures compared to the wild-type plants (Fig. S7). However, when subjected to drought, both *GC1::ACA11* lines displayed higher leaf temperatures compared to wild-

type plants (Fig. S7). This difference in temperature indicates that the *GC1::ACA11* leaves have the ability to reduce transpirational water loss in response to water stress. Supporting this notion, the water loss from detached leaves in *GC1::ACA11* plants was significantly lower than that in wild-type plants (Fig. 5D). Altogether, these findings strongly suggest that overexpression of *ACA11* enables stomatal closure and efficiently mitigates water loss during drought periods, thereby significantly enhancing drought tolerance.

Modelling prediction and experimental validation confirm overexpression of tonoplast Ca^{2+}-ATPase promoting ABA-evoked $[Ca^{2+}]_i$ elevation

The strong drought tolerance observed in *GC1::ACA11* plants prompted us to investigate their responsiveness to ABA. To achieve this, we applied OnGuard once again to analyse the stomatal response to ABA. Following the previously described method (Nguyen et al., 2023), we simulated the response of both the wild-type and *ox tACA* plants to ABA (Appendix A3). Fig. 6A illustrates the simulated changes in stomatal aperture in both wild-type and *ox tACA* plants in response to 1μM ABA. Interestingly, the closure of stomatal aperture in the *ox tACA* plants was more than 10% greater compared to the wild-type (Fig 6A and B). Microscopic outputs from OnGuard demonstrated the ABA response of overexpressing tonoplast Ca^{2+}-ATPase on the major ion fluxes in guard cell (Fig. 6 and Fig. S8-S12). Generally, the overexpression of tonoplast Ca^{2+}-ATPase led to an increase in ABA-induced $[Ca^{2+}]_i$ elevation (Fig 6A and Fig. S12). The maximum $[Ca^{2+}]_i$ levels in *ox tACA* plants were significantly higher than those in the wild-type (Fig. 6A and B). The elevated $[Ca^{2+}]_i$ promotes larger K^+ and Cl^- effluxes than wild-type plants (Fig. S9 and S10), which dramatically decrease guard cell turgor pressure and close the stomatal aperture. Overall, our modelling results predict that the overexpression of Ca^{2+}-ATPase leads to significant changes in $[Ca^{2+}]_i$, which subsequently impact stomatal closure in response to ABA.

To validate these predictions, we first examined the ABA-induced closure of stomata in both wild-type and *GC1::ACA11* plants. Fig. 7A demonstrates the effects of 20 μM ABA on stomatal closure over a 30-minute timeframe in these plants. The

GC1::ACA11 plants displayed faster stomatal closure compared to wild-type plants exposed to 20 μM ABA, and their stomata exhibited a greater degree of closure over a longer period (Fig. 7A). To investigate whether the difference in ABA-induced stomatal closure between the two plant types is influenced by $[Ca^{2+}]_i$, we conducted experiments using La^{3+} (a plasma membrane channel blocker) and BAPTA-AM (a calcium chelator that can penetrate the cytosol). In response to ABA, we found that both plant types were still able to close their stomata when treated with La^{3+} (Fig. 7B). However, the *GC1::ACA11* plants exhibited a higher degree of stomatal closure (Fig. 7B). On the other hand, pretreatment with BAPTA-AM resulted in only marginal changes in stomatal closure for both the wild-type and *GC1::ACA11* plants (Fig. 7C). These suggest that the difference in ABA-induced stomatal closure between the two plant types was predominantly influenced by $[Ca^{2+}]_i$ levels.

In order to investigate the influence of overexpressing ACA11 on ABA-induced changes in $[Ca^{2+}]_i$, we created the *GC1::ACA11* plants with Ca^{2+} indicator YC3.6. The results showed significant differences, as the *GC1::ACA11-YC3.6* plants exhibited a noticeable increase in $[Ca^{2+}]_i$ compared to the wild-type plants (Fig. 7D). To further confirm our findings, we employed fluorescence ratio imaging and loaded the Ca^{2+}-sensitive dye Fura2 to measure $[Ca^{2+}]_i$. Consistently, the *GC1::ACA11* plants displayed a remarkable elevation in $[Ca^{2+}]_i$ in response to ABA, with mean values of 1408 ± 92 nM and 1368 ± 78 nM in the *GC1::ACA11* lines respectively (Fig. S13). These values were significantly higher than the mean value observed in the wild-type plants (Fig. S13). Therefore, our findings provide confirmation that the guard cells of the *GC1::ACA11* plants possess an enhanced ability to elevate $[Ca^{2+}]_i$ in response to ABA.

DISCUSSION

Overexpression of *ACA11* promotes Ca^{2+} sequestration affecting Ca^{2+} homeostasis

Ca^{2+} are widely recognized as ubiquitous second messengers in living organisms, spanning from plants to animals, and they play a significant role in various physiological and developmental processes (Blatt, 2000; Dodd et al., 2010; Kudla et al., 2018; Wang et al., 2018). In plants, despite their relatively low concentration in the

cytosol, Ca^{2+} can account for up to 5% of the plant's dry weight (White and Broadley, 2003). Specifically, in guard cells, which regulate stomatal opening and closing, the resting $[Ca^{2+}]_i$ levels usually range between 100-200 nM (Blatt, 2000). When $[Ca^{2+}]_i$ levels rise to the micromolar range, they have a significant impact on ion fluxes through anion channels, leading to stomatal closure (Blatt and Thiel, 1993; Blatt, 1999, 2000). This elevation in $[Ca^{2+}]_i$ is achieved through both Ca^{2+} entry across the plasma membrane and release from intracellular stores (Grabov and Blatt, 1999; Hamilton et al., 2000; Garcia-Mata et al., 2003; Wang et al., 2013). For instance, ABA activates a low-conductance Ca^{2+} channel at the plasma membrane, which is associated with reactive oxygen species, and strongly influences the voltage sensitivity for $[Ca^{2+}]_i$ increases (Grabov and Blatt, 1998, 1999; Hamilton et al., 2000; Hamilton et al., 2001; Kwak et al., 2003; Mori et al., 2004; Wang et al., 2013). The rise in $[Ca^{2+}]_i$, achieved through Ca^{2+} entry at the plasma membrane, further triggers Ca^{2+} release from intracellular stores, a phenomenon known as Ca^{2+}-induced Ca^{2+} release (Blatt, 2000; Jezek and Blatt, 2017).

Interestingly, it has been estimated that more than 95% of the Ca^{2+} entering the cytoplasm during $[Ca^{2+}]_i$ elevations originates from intracellular stores (Chen et al., 2012; Minguet-Parramona et al., 2016; Jezek et al., 2021), with vacuoles being the largest storage organelles in plant cells. Vacuoles serve as the primary reservoir for intracellular Ca^{2+} and play a crucial role in regulating $[Ca^{2+}]_i$. The main transporters responsible for sequestering Ca^{2+} influx into the vacuole are the high-affinity Ca^{2+}-ATPases located on the tonoplast. These Ca^{2+}-ATPases are naturally inhibited by an auto-inhibitory domain located at the N-terminus (Malmström et al., 1997; Harper et al., 1998). However, this inhibition is relieved upon binding of Ca^{2+}/calmodulin to the Ca^{2+}-ATPases (Tidow et al., 2012). Consequently, these Ca^{2+}-ATPases are crucial for maintaining cellular Ca^{2+} levels in balance (Geisler et al., 2000; McAinsh and Pittman, 2009; Garcia Bossi et al., 2020). During stomatal opening, the activation of plasma membrane H^+-ATPase by light results in a negative membrane voltage, which in turn triggers the influx of Ca^{2+} across the plasma membrane, leading to an increase in $[Ca^{2+}]_i$. Subsequently, Ca^{2+}-ATPases restore $[Ca^{2+}]_i$ levels back to their resting values and

transport Ca^{2+} into the vacuole, which then acts as a main source for regulated Ca^{2+} release (Evans and Williams, 1998; Sanders et al., 1999). In a recent study, the knockout of Ca^{2+}-ATPases *ACA4* and *ACA11* was found to impair Ca^{2+} sequestration, resulting in delayed Ca^{2+} cycling and altered stomatal responsiveness (Jezek et al., 2021). The reduced population of tonoplast Ca^{2+}-ATPases resulted in decreased Ca^{2+} release from the vacuole and $[Ca^{2+}]_i$ elevation. This study emphasizes the importance of efficient Ca^{2+} sequestration in determining the temporal characteristics of $[Ca^{2+}]_i$ increases.

In our study, we used OnGuard modeling to investigate the impact of overexpressing tonoplast Ca^{2+}-ATPases on $[Ca^{2+}]_i$ and Ca^{2+} storage in the vacuole (Fig. S1-S4). Although there are currently no direct methods available to measure guard cell vacuolar Ca^{2+} concentration, we have conducted indirect measurements on the total Ca^{2+} content in the guard cell protoplasts. The results of our study revealed a significant increase in the total Ca^{2+} content in *GC1::ACA11* guard cell protoplasts compared to the wild-type plants (Table S3). It is important to note that the vacuole constitutes approximately 90% of the guard cell volume, and the resting $[Ca^{2+}]_i$ is similar between wild-type and *GC1::ACA11* plants (Fig S13). These findings suggest that the overexpression of tonoplast Ca^{2+}-ATPases facilitates the storage of Ca^{2+} in the vacuoles. During the drought stress, the larger stored Ca^{2+} in the vacuole serves as the main source for continuous Ca^{2+} release, triggering an elevation in $[Ca^{2+}]_i$ and leading to a sharp closure of stomata, thus improving drought tolerance (Fig.6 and 7). Our results further reinforce the essential role of tonoplast Ca^{2+}-ATPase in Ca^{2+} store and maintaining cellular Ca^{2+} homeostasis. In line with Jezek *et al*. (Jezek et al., 2021) conclusion, it is important to not only focus on the pathway of Ca^{2+} entry through the plasma membrane, but also to acknowledge the crucial role of Ca^{2+} sequestration in elevating cellular Ca^{2+} levels.

Enhancing stomatal opening and drought tolerance can be achieved simultaneously

Stomata provide the major pathway for the diffusion of CO_2, O_2, and water vapor between the ambient atmosphere and the interior of the leaf, which is crucial for plant photosynthesis and transpiration. One approach to enhance photosynthesis and promote

plant growth is through genetically manipulation of transporters in the guard cells. For example, the elimination of the plasma membrane SLAC1 anion channel (Negi et al., 2008; Vahisalu et al., 2008), responsible for solute loss during stomatal closure, can increase stomatal aperture (Wang et al., 2012; Laanemets et al., 2013). However, these mutants exhibit less responsive to ABA, CO_2, and light, resulting in a larger stomatal opening and increased water loss (Yamamoto et al., 2016). Recent studies have found that the *slac1* mutant in rice exhibits higher rates of leaf photosynthesis but fails to improve yield (Kusumi et al., 2017; Yamori et al., 2020). This may be due to the constantly increased water loss that limits plant growth (Wang et al., 2022). Similarly, overexpression of the plasma membrane H^+-ATPase in guard cells has been found to promote stomatal opening and increase photosynthesis (Wang et al., 2014). However, despite similar drought tolerance to wild-type plants, the overexpression lines exhibit lower WUE.

Another primary method of modifying plant stomata is altering stomatal density to regulating water loss. Recent studies have focused on the overexpression of secreted epidermal patterning factor (EPF) peptides, such as EPF1 and EPF2, which have been shown to reduce stomatal density in many plant species (Franks et al., 2015; Bertolino et al., 2019; Wang et al., 2022). By genetically modifying these plants, they exhibited a significantly higher WUE while maintaining a slightly lower photosynthetic rate, indicating potential in improving drought tolerance and water conservation. Additionally, overexpressing the *SDD1* gene, a negative regulator of stomatal development, resulted in reduced stomatal density, leading to decreased water consumption and enhanced drought tolerance (Yoo et al., 2010). However, it is worth noting that increasing stomatal density, achieved through knockout of *EPF1* or overexpression of *STOMAGEN* (an EPF-like peptide), can significantly enhance stomatal conductance and leaf photosynthetic rate (Tanaka et al., 2013). Again, plants with higher stomatal density often suffer from poor WUE, which hinders the conversion of photosynthesis advantages into biomass.

Manipulating stomatal dynamics in response to light has recently been recognized as a promising option for improving photosynthesis and WUE (Lawson and Blatt, 2014;

Lawson and Vialet-Chabrand, 2019). One method involves the application of a synthetic K^+ channel called BLINK1 to accelerate the kinetics of stomatal opening and closing, offering a potential means to improve WUE without compromising carbon fixation under fluctuant light condition (Papanatsiou et al., 2019). Genetic variations in stomatal kinetics within a diverse range of rice genetics have revealed that increased expression of *OsNHX1* can enhance crop water use efficiency and biomass production under drought conditions (Qu et al., 2020). Unfortunately, there are limited strategies available to enhance both stomatal aperture and drought tolerance in plants simultaneously, especially under stable conditions.

Under the guidance of OnGuard, our study has successfully produced transgenic plants that overexpress the *ACA11* gene, which promotes stomatal opening and enhances plant growth. Similar to the overexpressing H^+-ATPase lines, the *GC1::ACA11* plants not only have larger stomatal apertures, which increase photosynthesis and enhance plant growth under normal conditions, but also exhibit lower WUE. However, in contrast to the overexpressing H^+-ATPase lines, the *GC1::ACA11* plants show improved drought tolerance by reducing water loss through their stomata. Further analysis revealed that the *GC1::ACA11* plants led to an enhanced burst of Ca^{2+} in response to ABA. This regulatory cascade finely tunes stomatal responses, ultimately resulting in improved drought tolerance. These findings highlight the potential of tonoplast-localized ACA11 in simultaneously enhancing stomatal opening and improving drought tolerance, making it a promising candidate for future applications in plant improvement.

The OnGuard model holds significant guidance for future design breeding

The mechanism of stomatal movement lends itself well to the "bottom-up" approach in quantitative system modelling. The OnGuard model is specifically designed to incorporate the biophysical and kinetic aspects of the transporters responsible for solute flux at the plasma membrane and tonoplast, which are crucial for stomatal movements (Chen et al., 2012; Hills et al., 2012; Rui et al., 2022). This model establishes connections between the activities of these transporters, considering factors such as membrane voltage, substrate concentration, and regulatory ligand concentrations that

occur *in vivo*. Importantly, the membrane voltage plays a vital role in the feedback loop between transporters, even within a single transporter. This allows the channel's activity to counteract its own flux based on intrinsic kinetic relations of the channel gating, without relying on external regulatory processes. By manipulating the characteristics of the transporters, the OnGuard model can produce counter-intuitive outputs, presenting unexpected results. This demonstrates the model's ability to simulate and study the intricate mechanism of stomatal movements.

In our study, we used *in silico* analysis to identify tonoplast Ca^{2+}-ATPases as a potential key target for enhancing stomatal aperture. It is important to note that manipulating a single transporter at a membrane does not only affect this specific process or the distribution of transported species alone. For instance, in the simulations on *slac* mutant, the elimination of the SLAC channel not only disrupted K^+ homeostasis and fluxes, but also had an impact on cytosolic Ca^{2+} and pH levels, which in turn affected stomatal behaviors in the *slac1* mutant (Wang et al., 2012). Similarly, in our study, we observed that overexpression of Ca^{2+}-ATPase led to an over-accumulation of Ca^{2+} in the vacuole, results in larger K^+ and Cl^- uptake into the cytosol that promote stomatal opening and reducing WUE. More important, this accumulated Ca^{2+} served as a primary resource for continuous release when need, ultimately resulting in stomatal closure and enhanced drought tolerance in plants. It is crucial to recognize that the consequences of such manipulations can be challenging to anticipate, often surpassing our intuitive understanding. Therefore, quantitative modeling is essential to effectively address these complex issues.

OnGuard has already yielded detail sufficient to guide phenotypic and mutational studies (Wang et al., 2012; Wang et al., 2017; Jezek et al., 2021; Horaruang et al., 2022; Nguyen et al., 2023), and it represents a key step toward 'reverse engineering' of stomatal guard cell physiology based on rational design and testing in simulation. Early studies have shown the potential to manipulate K^+ channel gating and populations to improve WUE (Wang et al., 2014), lead to the production of BLINK1 plants that improved WUE without compromising carbon fixation. Our study further highlights the importance of tonoplast Ca^{2+}-ATPase in balancing plant growth and drought

tolerance through *in silico* analysis, which was confirmed through experiments. The predictive capabilities of the OnGuard model are impressive, and it has the potential to guide plant improvement and breeding efforts. As breeding technology continues to advance, more tools are needed to assist in designing breeding strategies. The quantitative nature of the OnGuard model makes it an invaluable tool for addressing various fundamental aspects of stomatal and whole plant physiology. We are confident that OnGuard will continue to play a vital role in future breeding efforts, leveraging its strengths to help create plants that are better adapted to changing environmental conditions while meeting the increasing demand for food production.

MATERIALS AND METHODS

Plant growth and whole-plants physiology.

The transgenic and wild-type (*Arabidopsis* Col-0) plants were cultivated in short-day conditions with 100 μmol m^{-2} s^{-1} light intensity, 22°C/18°C (day/night) temperature, and 55%/70% relative humidity. Two weeks following germination, seedlings were moved to 5 cm pots for a four-week period in order to analyze rosette area, biomass, and WUE. Rosette areas were analysed from calibrated pictures and were harvested, fresh and dry weights calculated as before. (Papanatsiou et al., 2019; Jezek et al., 2021). The amount of water used was tracked during the trial. The formula used to calculate the whole plant's WUE was WUE = dry weight (g)/water consumption (L). For drought treatment, seedlings were transferred to the same pot for two weeks after germination and subjected to water stress for 20 days. After the water stress period, the plants were re-watered for an additional one week to observe their recovery.

Gas exchange measurement.

The LI-COR 6800 systems were used to measure gas exchange, following the previously described methods (Wang et al., 2012; Wang et al., 2017; Jezek et al., 2021). All plants were examined at least three different times throughout the same phase of the relative diurnal cycle in order to guarantee consistency. For light response curves, plants were given an initial 30 min of high-light (1500 μmol m^{-2} s^{-1} PAR) adaptation, and then the light intensity gradually decreased from 1500 to 0 μmol m^{-2} s^{-1} PAR in

steps lasting more than 3 minutes (stable state). The leaves were first acclimated to an ambient CO_2 (C_a) of 400 μmol mol^{-1} under 1000 m^{-2} s^{-1} PAR light intensity in order to create the CO_2 response curves. The C_a concentration was then changed stepwise from 400 to 1200 μmol mol^{-1}, with intervals of 3 minutes.

Water loss calculation.

To calculate water loss, leaves from four-week-old plants that had been well-watered were dried in a controlled laboratory setting and weighed using a microbalance every 30 min. The water loss was calculated as the percentage of (starting fresh weight - fresh weight at every interval) divided by the starting fresh weight.

Construction of the overexpression vector and transgenic plants.

The Gateway-compatible vectors used for plant transformation were constructed using Restriction and Insertion cloning, and NEBuilder® HiFi DNA Assembly (New England Biolabs, UK). Briefly, the ubiquitin 10 (UBQ10) promoter region of vector sets (Grefen et al., 2010) were replaced by GC1 promoter. For pGC1N-GFP-Dest, a 1,725 DNA fragment of the GC1 promoter was amplified from pPZP211-GC1(Wang et al., 2014) with following primers 5'-gcggagctcggctacaagaagagtaaagatt-3' and 5'-cgcctcgagatttcttgagtagtgattttgaa-3' flanked by SacI and XhoI sites to replace the corresponding regions of UBQ10 in pUBN-GFP-Dest (Grefen et al., 2010). For pGC1-Dest, pUB-Dest was linearized with EcoRI before NEBuilder® HiFi DNA Assembly reaction. Insertion fragments were amplified from pPZP211-GC1 and pUB-Dest, respectively, with following primers: 5'-cagctatgaccatgattacgaattcGAGCTCGGCTACAAGAAG-3' and 5'-cgcactcgagATTTCTTGAGTAGTGATTTTGAAG-3' for GC1 promoter, 5'-ctcaagaaatCTCGAGTGCGGGATCCTC-3' and 5'-cgtctttcattgccatacggaattcCGGATGAGCATTCATCAGG-3' for 476 bp DNA fragment of Gateway cassette. Linearized vectors with two fragments were assembly following manufacture's suggestion to construct pGC1-Dest. For pGC1C-GFP-Dest, pUBC-GFP-Dest was linearized with SacI and XhoI sites and the 3541 bp DNA fragments of GC1 promoter and Gateway cassette were amplified from pGC1-Dest with following primers: 5'-catgattacgaattcgagctcGGCTACAAGAAGAGTAAAGATTC-3' and 5'-

caccatactagttggatatctcgagTCGACACGCGTAGATCTC-3' for NEBuilder® HiFi DNA Assembly reaction. The open-reading frame of *ACA11* was amplified and inserted into pGC1 vectors. After sequencing, the vectors were used for transformation of *Arabidopsis* Col-0 and the YC3.6 lines using Agrobacterium-mediated transformation. Two independent homozygous T_3 lines (*GC::ACA11*#1 and *GC::ACA11*#2) were used for all phenotypic analyses and two *GC::ACA11-YC3.6* (*GC::ACA11*#1-YC3.6 and *GC::ACA11*#2-YC3.6) lines were used to measure the changes in $[Ca^{2+}]_i$.

Gene expression analysis

Total RNA was extracted from mature leaves, and transcript levels were examined using quantitative PCR in the same manner (Wang et al., 2012). Special primers (Table S4) were created for the plasma membrane and tonoplast key transporters. Internal controls were provided by the *ACT2* actin and *TUB9* tubulin genes.

Stomatal assay.

In freshly expanded leaf epidermal peels, stomatal apertures were measured. After being removed from the abaxial leaf surface, the peels were submerged in various solutions. 10 mM KCl and 5 mM MES titrated with $Ca(OH)_2$ to its pKa of 6.1 (1 mM $[Ca^{2+}]$) were present in the standard perfusion buffer. In experiments with ABA treatments, the experiment was carried out after mixing 20 μM ABA with standard buffer. In experiments with Ca^{2+} measurement, peels were preincubated with the standard buffer with 100 μM $LaCl_3$ and/or 25 μM BAPTA-AM. Measurements were made with an HD digital camera at 5-min intervals. After calibration, stomatal apertures were calculated offline using ImageJ (v.1.51h).

Stomatal density was calculated according to a previous method (Wang et al., 2014b). Three expanded leaves from each plant were selected. Three microphotographs were randomly taken from the same area of each collected leaf. To quantify the stomatal density, the number of stomata present in each microphotograph was meticulously counted.

Thermal imaging

Using a thermography infrared camera (FLIR A300), thermal pictures of the plants were taken under both normal and drought conditions. To ensure accurate observations, the camera was positioned vertically, about one meter above the leaf canopy.

$[Ca^{2+}]_i$ recording

Fura2 fluorescence ratio imaging using a cooled Pentamax-512 CCD camera and GenIV intensifier (Princeton Instruments) was used to determine [Ca2+]i, as previously mentioned (Wang et al., 2012; Wang et al., 2013; Wang et al., 2017; Jezek et al., 2021).Fluorescence picture pairs were excited with 340- and 390-nm light (10-nm slit width; Polychrom II; Til Photonics) and then collected at 2-, 5-, and 10-s intervals using a 535-nm interference filter (620 nm bandwidth). Using MetaFluor and MetaMorph software version 6.1 (Universal Imaging), images were adjusted for background fluorescence that was captured prior to dye loading, and fluorescence and fluorescence ratios were examined.

To detect fluorescence signals emitted by the YC3.6 indicator in guard cell, a confocal microscope (Olympus FV3000) was employed. The excitation wavelength used was 445 nm, and the emission wavelengths were set to detect CFP at 485/40 nm and YFP at 535/30 nm. Images were acquired every 6 seconds for a total duration of 25 minutes. To analyze the changes in $[Ca^{2+}]_i$, we examined the ratio of YFP to CFP fluorescence intensities in the acquired images using ImageJ software (v.1.51h).

Isolation of guard cell protoplasts

Guard cell protoplasts mesophyll cell protoplasts were separated from *Arabidopsis* wild-type and *GC1::ACA11* plants' rosette leaves using the techniques described in Ueno et al. (2005) and Hayashi et al. (2017). Guard cell protoplasts and mesophyll cell protoplasts were collected, and they were freeze-dried before being used.

Element analysis with ICP-MS

The freeze-dried protoplasts were digested in PFA vessels with 1.5 ml of 65% HNO_3 and 0.6 ml of 30% H_2O_2 for 15 min at 170 °C in a DTU-2CN nitric acid digestion furnace (TAITEC, Japan). Upon cooling to room temperature, the digested solution was transferred to a plastic volumetric flask and diluted to 5 ml with deionized water. The

calcium content was determined using ICP-MS (iCAP RQ, Thermo Fisher Scientific, USA).

OnGuard modelling

Built on the HoTSig platform, OnGuard3 (Jezek et al., 2021) features the extension of OnGuard2 (Wang et al., 2017) for stomatal transpiration, distinct assignments of blue and red light, and the limitation imposed by surrounding cells on the guard cells. Every model output was obtained from the diurnal light-dark cycle that the OnGuard3 models were driven through, with increments in light imposed on it as shown. The guard cell's primary, energy-dependent transport, sucrose and malic acid production, and light-induced apoplastic solute contents were all determined to remain constant (Jezek et al., 2019; Jezek et al., 2021; Nguyen et al., 2023). According to Shafaque et al. (2020) and Jezek et al. (2021), all other model parameters were fixed. Thus, the properties of individual transporters, metabolism, and buffering reactions responded solely to changes in model variables influenced by the encoded parameters.

Statistics

The results of the study are presented as means ± SE of n observations, and the student t test is used to assess significance. It is significant to remember that models like the OnGuard model, which are based on ordinary differential equations, are capable of consistently replicating a specific set of outputs using the same model parameters. Consequently, conducting statistical analysis on these outputs becomes irrelevant.

ACKNOWLEDGEMENTS

This work was supported by the Zhejiang Provincial Natural Science Foundation (LR21C020001), National Natural Science Foundation of China (32372017, 31871537 and U2003115) and Hainan Seed Industry Laboratory (B21HJ0220) to Y. W.; the Biotechnology and Biological Sciences Research Council (BBSRC) grants (BB/W001217/1) to M. R. B. and R. K.; the BBSRC grants (BB/S017348/1) and Royal Society University Research Fellowship awards (URF\R\211002) to R. K.

CONFLICTS OF INTEREST

The authors declare that they have no conflict of interest.

AUTHOR CONTRIBUTIONS

Y. W. conceived the idea of this study and designed research. L. X., R. K. and M. R. B. design the vectors. J.S., B. H., B. Y., Q. C., Y. J. and P. L. performed experiments and analysed data. P.L., D. X. and Y.W. wrote the manuscript.

REFERENCES

Bertolino L.T., Caine R.S., Gray J.E. (2019) Impact of stomatal density and morphology on water-use efficiency in a changing world. Front. Plant Sci. **10**: 225.

Blatt M.R. (1999) Reassessing roles for Ca^{2+} in guard cell signalling. J. Exp. Bot. **50:** 989-999.

Blatt M.R. (2000) Ca^{2+} signalling and control of guard-cell volume in stomatal movements. Curr. Opin. Plant Biol. **3:** 196-204.

Blatt M.R., Brodribb T.J., Torii K.U. (2017) Small pores with a big impact. Plant Physiol. **174:** 467-469.

Blatt M.R., Jezek M., Lew V.L., Hills A. (2022) What can mechanistic models tell us about guard cells, photosynthesis, and water use efficiency? Trends in Plant Sci. **27:** 166-179.

Blatt M.R., Thiel G. (1993) Hormonal-control of ion channel gating. Annu. rev. Plant Physiol. Plant Mol. Biol. **44:** 543-567.

Bossi J.G., Kumar K., Barberini M.L., Dominguez G.D., Guerrero Y.D.C.R., Marino-Buslje C., Obertello M., Muschietti J.P., Estevez J.M. (2020) The role of P-type IIA and P-type IIB Ca^{2+}-ATPases in plant development and growth. J. Exp. Bot. **71:** 1239-1248.

Boursiac Y., Lee S.M., Romanowsky S., Blank R., Sladek C., Chung W.S., Harper J.F. (2010) Disruption of the vacuolar calcium-ATPases in *Arabidopsis* results in the activation of a salicylic acid-dependent programmed cell death pathway. Plant Physiol. **154:** 1158-1171.

Chen Z.H., Hills A., Baetz U., Amtmann A., Lew V.L., Blatt M.R. (2012) Systems dynamic modeling of the stomatal guard cell predicts emergent behaviors in transport, signaling, and volume control. Plant Physiol. **159:** 1235-1251.

Dodd A.N., Kudla J., Sanders D. (2010) The language of calcium signaling. Annu. Rev. Plant Biol. **61:** 593-620.

Evans D.E., Williams L.E. (1998) P-type calcium ATPases in higher plants - biochemical, molecular and functional properties. Biochimica Et Biophysica Acta-Reviews on Biomembranes **1376:** 1-25.

Franks P.J., Doheny-Adams T.W., Britton-Harper Z.J., Gray J.E. (2015) Increasing water-use efficiency directly through genetic manipulation of stomatal density. New Phytol. **207:** 188-195.

Garcia-Mata C., Gay R., Sokolovski S., Hills A., Lamattina L., Blatt M.R. (2003) Nitric oxide regulates K^+ and Cl^- channels in guard cells through a subset of abscisic acid-evoked signaling pathways. Proc. Natl. Acad. Sci. **100:** 11116-11121

Geisler M., Axelsen K.B., Harper J.F., Palmgren M.G. (2000) Molecular aspects of higher plant P-type Ca^{2+}-ATPases. Biochimica Et Biophysica Acta-Biomembranes **1465:** 52-78.

Geisler M., Frangne N., Gomès E., Martinoia E., Palmgren M.G. (2000) The *ACA4* gene of *Arabidopsis* encodes a vacuolar membrane calcium pump that improves salt tolerance in yeast. Plant Physiol. **124:** 1814-1827.

Grabov A., Blatt M.R. (1998) Membrane voltage initiates Ca^{2+} waves and potentiates Ca^{2+} increases with abscisic acid in stomatal guard cells. Proc. Natl. Acad. Sci. **95:** 4778-4783.

Grabov A., Blatt M.R. (1999) A steep dependence of inward-rectifying potassium channels on cytosolic free calcium concentration increase evoked by hyperpolarization in guard cells. Plant Physiol. **119:** 277-287.

Grefen C., Donald N., Hashimoto K., Kudla J., Schumacher K., Blatt M.R. (2010) A ubiquitin-10 promoter-based vector set for fluorescent protein tagging facilitates temporal stability and native protein distribution in transient and stable expression studies. Plant J. **64:** 355-365.

Gupta A., Rico-Medina A., Cano-Delgado A.I. (2020) The physiology of plant responses to drought. Science **368:** 266-269.

Hamilton D.W.A., Hills A., Blatt M.R. (2001) Extracellular Ba^{2+} and voltage interact to gate Ca^{2+} channels at the plasma membrane of stomatal guard cells. FEBS Lett. **491:** 99-103.

Hamilton D.W.A., Hills A., Kohler B., Blatt M.R. (2000) Ca^{2+} channels at the plasma membrane of stomatal guard cells are activated by hyperpolarization and abscisic acid. Proc. Natl. Acad. Sci. **97:** 4967-4972.

Harper J.F., Hong B., Hwang I., Guo H.Q., Stoddard R., Huang J.F., Palmgren M.G., Sze H. (1998) A novel calmodulin-regulated Ca^{2+}-ATPase (ACA2) from *Arabidopsis* with an N-terminal autoinhibitory domain. J Biol Chem. 273(2):1099–1106.

Hayashi M., Inoue S., Ueno Y., Kinoshita T. (2017) A Raf-like protein kinase BHP mediates blue light-dependent stomatal opening. Sci. Rep. 7: 45586.

Hetherington A.M., Woodward F.I. (2003) The role of stomata in sensing and driving environmental change. Nature **424:** 901-908.

Hills A., Chen Z.H., Amtmann A., Blatt M.R., Lew V.L. (2012) OnGuard, a computational platform for quantitative kinetic modeling of guard cell physiology. Plant Physiol. **159:** 1026-1042.

Horaruang W., Klejchova M., Carroll W., Silva-Alvim F.A.L., Waghmare S., Papanatsiou M., Amtmann A., Hills A., Alvim J.C., Blatt M.R., Zhang B. (2022) Engineering a K^+ channel 'sensory antenna' enhances stomatal kinetics, water use efficiency and photosynthesis. Nat. Plants **8:** 1262-1274.

Hosy E., Vavasseur A., Mouline K., Dreyer I., Gaymard F., Porée F., Boucherez J., Lebaudy A., Bouchez D., Véry A.A., Simonneau T., Thibaud J.B., Sentenac H. (2003) The *Arabidopsis* outward K^+ channel *GORK* is involved in regulation of stomatal movements and plant transpiration. Proc. Natl. Acad. Sci. **100:** 5549-5554.

Jezek M., Blatt M.R. (2017) The membrane transport system of the guard cell and its integration for Stomatal Dynamics. Plant Physiol. **174:** 487-519.

Jezek M., Hills A., Blatt M.R., Lew V.L. (2019) A constraint-relaxation-recovery mechanism for stomatal dynamics. Plant Cell Environ. **42:** 2399-2410.

Jezek M., Silva-Alvim F.A.L., Hills A., Donald N., Ishka M.R., Shadbolt J., He B., Lawson T., Harper J.F., Wang Y., Lew V.L., Blatt M.R. (2021) Guard cell endomembrane Ca^{2+}-ATPases underpin a 'carbon memory' of photosynthetic assimilation that impacts on water-use efficiency. Nat. Plants **7:** 1301-1313.

Kim T.H., Bohmer M., Hu H.H., Nishimura N., Schroeder J.I. (2010) Guard cell signal transduction network: Advances in understanding abscisic acid, CO_2, and Ca^{2+} signaling. Annu. Rev. Plant Biol. **61:** 561-591.

Kudla J., Becker D., Grill E., Hedrich R., Hippler M., Kummer U., Parniske M., Romeis T., Schumacher K. (2018) Advances and current challenges in calcium signaling. New Phytol. **218:** 414-431.

Kusumi K., Hashimura A., Yamamoto Y., Negi J., Iba K. (2017) Contribution of the S-type Anion Channel SLAC1 to Stomatal Control and Its Dependence on Developmental Stage in Rice. Plant Cell Physiol. **58:** 2085-2094.

Kwak J.M., Mori I.C., Pei Z.M., Leonhardt N., Torres M.A., Dangl J.L., Bloom R.E., Bodde S., Jones J.D.G., Schroeder J.I. (2003) NADPH oxidase *AtrbohD* and *AtrbohF* genes function in ROS-dependent ABA signaling in *Arabidopsis*. Embo J. **22:** 2623-2633.

Laanemets K., Wang Y.F., Lindgren O., Wu J.Y., Nishimura N., Lee S., Caddell D., Merilo E., Brosche M., Kilk K., Soomets U., Kangasjarvi J., Schroeder J.I., Kollist H. (2013) Mutations in the SLAC1 anion channel slow stomatal opening and severely reduce K^+ uptake channel activity via enhanced cytosolic Ca^{2+} and increased Ca^{2+} sensitivity of K^+ uptake channels. New Phytol. **197:** 88-98.

Lawson T., Blatt M.R. (2014) Stomatal size, speed, and responsiveness impact on photosynthesis and water use efficiency. Plant Physiol.**164:** 1556-1570.

Lawson T., Vialet-Chabrand S. (2019) Speedy stomata, photosynthesis and plant water use efficiency. New Phytol. **221:** 93-98.

Lawson T., von Caemmerer S., Baroli I. (2011) Photosynthesis and stomatal behaviour. *In* U Luttge, W Beyschlag, B Budel, D Francis, eds, Progress in Botany 72, Vol 72, pp 265-304.

Lee S.C., Luan S. (2012) ABA signal transduction at the crossroad of biotic and abiotic stress responses. Plant Cell Environ. **35:** 53-60.

Lee S.M., Kim H.S., Han H.J., Moon B.C., Kim C.Y., Harper J.F., Chung W.S. (2007) Identification of a calmodulin-regulated autoinhibited Ca^{2+}-ATPase (ACA11) that is localized to vacuole membranes in *Arabidopsis*. FEBS Lett. **581:** 3943-3949.

Malmström S., Askerlund P., Palmgren M.G. (1997). A calmodulin-stimulated Ca^{2+}-ATPase from plant vacuolar membranes with a putative regulatory domain at its N-terminus. FEBS Lett. 400(3):324–328.

McAinsh M.R., Pittman J.K. (2009) Shaping the calcium signature. New Phytol. **181:** 275-294.

Minguet-Parramona C., Wang Y., Hills A., Vialet-Chabrand S., Griffiths H., Rogers S., Lawson T., Lew V.L., Blatt M.R. (2016) An optimal frequency in Ca^{2+} oscillations for stomatal closure is an emergent property of ion transport in guard cells. Plant Physiol. **170:** 33-42.

Mori I.C., Kwak J.M., Leonhardt N., Bloom R., Bodde S., Schroeder J.I. (2004) Reactive oxigen species regulation in ABA signaling in *Arabidopsis* guard cells. Plant Cell Physiol. **45:** S52-S52.

Munemasa S., Hauser F., Park J., Waadt R., Brandt B., Schroeder J.I. (2015) Mechanisms of abscisic acid-mediated control of stomatal aperture. Curr. Opin. Plant Biol. **28:** 154-162.

Negi J., Matsuda O., Nagasawa T., Oba Y., Takahashi H., Kawai-Yamada M., Uchimiya H., Hashimoto M., Iba K. (2008) CO_2 regulator SLAC1 and its homologues are essential for anion homeostasis in plant cells. Nature **452:** 483-486.

Nguyen T.H., Silva-Alvim F.A.L., Hills A., Blatt M.R. (2023) OnGuard3e: A predictive, ecophysiology-ready tool for gas exchange and photosynthesis research. Plant Cell Environ. **46:** 3644-3658.

Papanatsiou M., Petersen J., Henderson L., Wang Y., Christie J.M., Blatt M.R. (2019) Optogenetic manipulation of stomatal kinetics improves carbon assimilation, water use, and growth. Science **363:** 1456-1459.

Pilot G., Gaymard F., Mouline K., Chérel I., Sentenac H. (2003) Regulated expression of *Arabidopsis* Shaker K^+ channel genes involved in K^+ uptake and distribution in the plant. Plant Mol. Biol. **51:** 773-787.

Qu M., Essemine J., Xu J., Ablat G., Perveen S., Wang H., Chen K., Zhao Y., Chen G., Chu C., Zhu X. (2020) Alterations in stomatal response to fluctuating light increase biomass and yield of rice under drought conditions. Plant J. **104:** 1334-1347.

Rui M., Jing Y., Jiang H., Wang Y. (2022) Quantitative system modeling bridges the gap between macro- and microscopic stomatal model. Adv. Biol. **6**: 2200131.

Sanders D., Brownlee C., Harper J.F. (1999) Communicating with calcium. Plant Cell **11:** 691-706.

Shafaque S., Ma Y., Rui M., He B., Zhu Z., Cao F., Wu F., Wang Y. (2020) Optimized protocol for OnGuard2 software in studying guard cell membrane transport and stomatal physiology. Front. Plant Sci. **11**: 131.

Tanaka Y., Sugano S.S., Shimada T., Hara-Nishimura I. (2013) Enhancement of leaf photosynthetic capacity through increased stomatal density in *Arabidopsis*. New Phytol. **198:** 757-764.

Tidow H., Poulsen L.R., Andreeva A., Knudsen M., Hein K.L., Wiuf C., Palmgren M.G., Nissen P. (2012). A bimodular mechanism of calcium control in eukaryotes. Nature, 491(7424):468-472.

Ueno K., Kinoshita T., Inoue S., Emi T., Shimazaki K. (2005) Biochemical characterization of plasma membrane H^+-ATPase activation in guard cell protoplasts of *Arabidopsis* thaliana in response to blue light. Plant Cell Physiol. 46(6): 955-963.

Vahisalu T., Kollist H., Wang Y.F., Nishimura N., Chan W.Y., Valerio G., Lamminmaki A., Brosche M., Moldau H., Desikan R., Schroeder J.I., Kangasjarvi J. (2008) SLAC1 is required for plant guard cell S-type anion channel function in stomatal signalling. Nature **452:** 487-491.

Wang Y., Blatt M.R., Chen Z.H. (2018) Ion transport at the plant plasma membrane. *In* eLS. John Wiley & Sons, Ltd: Chichester.

Wang Y., Chen Z.H., Zhang B., Hills A., Blatt M.R. (2013) PYR/PYL/RCAR abscisic acid receptors regulate K^+ and Cl^- channels through reactive oxygen species-mediated activation of Ca^{2+} channels at the plasma membrane of intact *Arabidopsis* guard cells. Plant Physiol. **163:** 566-577.

Wang Y., Hills A., Blatt M.R. (2014a) Systems analysis of guard cell Membrane transport for enhanced stomatal dynamics and water use efficiency. Plant Physiol. **164:** 1593-1599.

Wang Y., Hills A., Vialet-Chabrand S., Papanatsiou M., Griffiths H., Rogers S., Lawson T., Lew V.L., Blatt M.R. (2017) Unexpected connections between humidity and ion transport discovered using a model to bridge guard cell-to-leaf scales. Plant Cell **29:** 2921-2939.

Wang Y., Noguchi K., Ono N., Inoue S.i., Terashima I., Kinoshita T. (2014b) Overexpression of plasma membrane H^+-ATPase in guard cells promotes light-induced stomatal opening and enhances plant growth. Proc. Natl. Acad. Sci. **111:** 533-538.

Wang Y., Papanatsiou M., Eisenach C., Karnik R., Williams M., Hills A., Lew V.L., Blatt M.R. (2012) Systems dynamic modeling of a guard cell Cl^- channel mutant uncovers an emergent homeostatic network regulating stomatal transpiration. Plant Physiol. **160:** 1956-1967.

Wang Y., Wang Y., Tang Y., Zhu X.G. (2022) Stomata conductance as a goalkeeper for increased photosynthetic efficiency. Curr. Opin. Plant Biol. **70:** 102310-102310.

White P.J., Broadley M.R. (2003) Calcium in plants. Ann. Bot. **92:** 487-511.

Yamamoto Y., Negi J., Wang C., Isogai Y., Schroeder J.I., Iba K. (2016) The transmembrane region of guard cell SLAC1 channels perceives CO_2 signals via an ABA-independent pathway in *Arabidopsis*. Plant Cell **28:** 557-567.

Yamori W., Kusumi K., Iba K., Terashima I. (2020) Increased stomatal conductance induces rapid changes to photosynthetic rate in response to naturally fluctuating light conditions in rice. Plant Cell Environ. **43:** 1230-1240.

Yoo C.Y., Pence H.E., Jin J.B., Miura K., Gosney M.J., Hasegawa P.M., Mickelbart M.V. (2010) The *Arabidopsis* GTL1 transcription factor regulates water use efficiency and drought tolerance by modulating stomatal density via transrepression of *SDD1*. Plant Cell **22:** 4128-4141.

SUPPORTING INFORMATIONS

802 **Appendix A1.** OnGuard model parameters for wild-type and mutants with ×2 and ×0.5
803 transporters' population
804 **Appendix A2.** OnGuard model parameters for wild-type and ox tACA plants
805 **Appendix A3.** OnGuard model parameters for wild-type and ox tACA plants in
806 response to ABA
807 **Table S1.** OnGuard model predicts the maximum aperture (Ap_{max}) and the minimum
808 aperture (Ap_{min}) by manipulation of transporter's population.
809 **Table S2.** Stomatal density of wild-type and *GC1::ACA11* transgenic plants.
810 **Table S3.** The total Ca^{2+} content of protoplasts from both wild-type and *GC1::ACA11*
811 transgenic plants
812 **Table S4.** Primers used for quantitative PCR analysis of transcript abundance.
813 **Figure S1.** *ACA 11* is specific expressed in guard cells driven by the GC1 promoter.
814 **Figure S2.** Relative transcript levels for selected plasma membrane and tonoplast
815 transporters from *GC1::ACA11* lines assayed by quantitative PCR.
816 **Figure S3.** Analysis of K^+ fluxes at the plasma membrane and tonoplast from the
817 OnGuard model in simulation of wild-type and *ox tACA* plants.
818 **Figure S4.** Analysis of Cl^- fluxes at the plasma membrane and tonoplast from the
819 OnGuard model in simulation of wild-type and *ox tACA* plants.
820 **Figure S5.** Analysis of H^+ fluxes at the plasma membrane and tonoplast from the
821 OnGuard model in simulation of wild-type and *ox tACA* plants.
822 **Figure S6.** Analysis of Ca^{2+} fluxes at the plasma membrane and tonoplast from the
823 OnGuard model in simulation of wild-type and *ox tACA* plants.
824 **Figure S7.** Thermal infrared imaging of wild-type and *GC1::ACA11* lines.
825 **Figure S8.** Analysis of voltage changes at the plasma membrane and tonoplast from
826 the OnGuard model in simulation of wild-type and *ox tACA* plants in response to
827 ABA.
828 **Figure S9.** Analysis of K^+ fluxes at the plasma membrane and tonoplast from the
829 OnGuard model in simulation of wild-type and *ox tACA* plants in response to ABA.
830 **Figure S10.** Analysis of Cl^- fluxes at the plasma membrane and tonoplast from the
831 OnGuard model in simulation of wild-type and *ox tACA* plants in response to ABA.
832 **Figure S11.** Analysis of H^+ fluxes at the plasma membrane and tonoplast from the
833 OnGuard model in simulation of wild-type and *ox tACA* plants in response to ABA.
834 **Figure S12.** Analysis of Ca^{2+} fluxes at the plasma membrane and tonoplast from the
835 OnGuard model in simulation of wild-type and *ox tACA* plants in response to ABA.

Figure S13. $[Ca^{2+}]_i$ recorded from wild-type and *GC1::ACA11* guard cells pre-loaded with the Ca^{2+}-sensitive fluorescent dye Fura2.

FIGURE LENGENDS

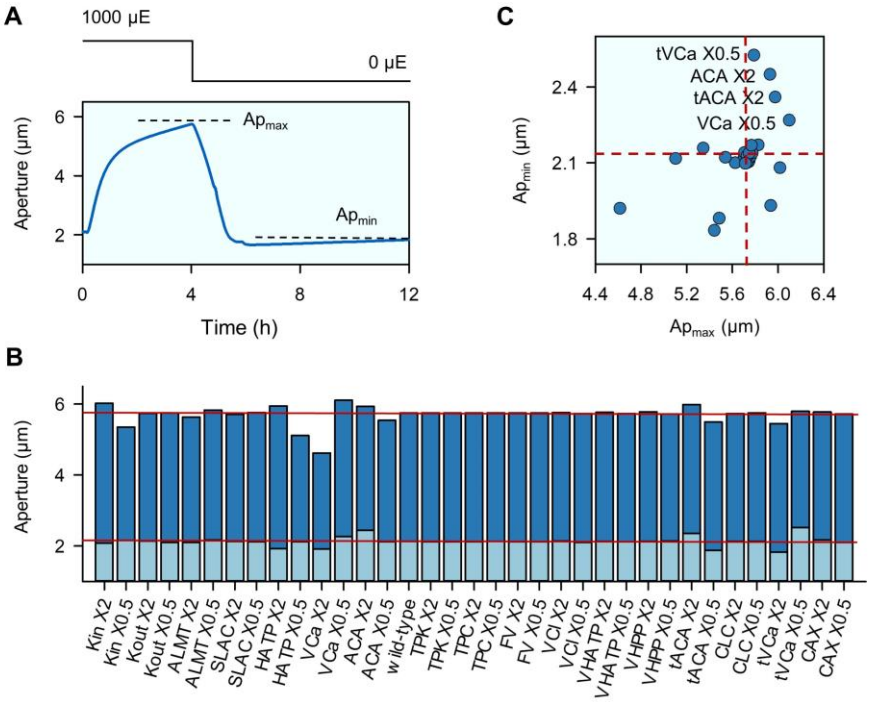

Figure 1. Manipulating transporter population identifies overexpressing tonoplast Ca^{2+}-ATPase that strongly influences stomatal aperture.

(A) Aperture dynamics, 24-h cycles (data shown for 12-h period) of stomatal opening and closing simulated under control conditions. Analysis parameters of the maximum aperture (Ap_{max}) and the minimum aperture (Ap_{min}) as indicated. **(B)** Dynamic range of apertures on increasing by 2-fold and reducing to 50% the population of each transporter. Red lines indicate the dynamic range of the control simulation (wild-type) for comparison. **(C)** The plots indicate the top impactor on Ap_{max} and Ap_{min} with increasing or decreasing population of each transporter on plasma membrane and tonoplast. Red lines indicate the range of the control simulation (wild-type) for comparison. Transporters at the plasma membrane are as follows: HATP, H^+-ATPase; Kin, inward-rectifier K^+ channel (KAT); Kout, outward-rectifier K^+ channel (GORK); ALMT, R-type anion channel; SLAC, S-type anion channel; VCa, voltage-gated (inward-rectifying) Ca^{2+} channel; ACA, Ca^{2+}-ATPase. Transporters at the tonoplast are as follows: TPC, TPC1- type cation channel; TPK, TPK1-type K^+ channel; FV, FV-

857 type K^+ channel; VCl, voltage-gated (inward-rectifying) Cl^- channel; VHATP, V-type
858 H^+-ATPase; VHPP, H^+-PPase; tACA, tonoplast Ca^{2+}-ATPase; CLC, CLC-type H^+-Cl^-
859 antiporter; tVCa, tonoplast voltage- and Ca^{2+}-gated Ca^{2+} channel; CAX, Ca^{2+}-H^+
860 antiporter.
861

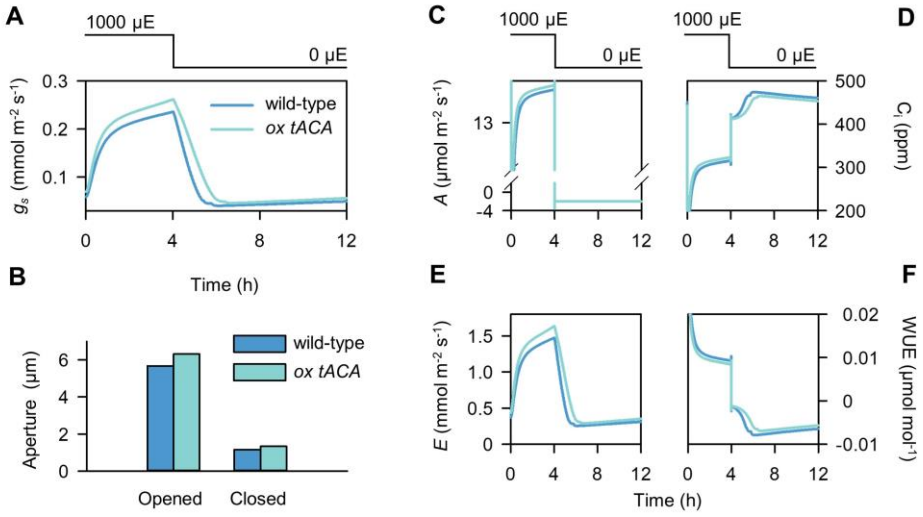

862

863 **Figure 2. Macroscopic outputs derived from the OnGuard modelling of wild-type**
864 **and *ox tACA* plants.**

865 (**A**-**F**) Stomatal conductance, g_s (**A**), stomatal aperture (**B**), Photosynthetic rate, *A* (**C**),
866 intracellular CO_2 concentration, C_i (**D**), transpiration, *E* (**E**) and water use efficiency,
867 WUE (**F**).

868

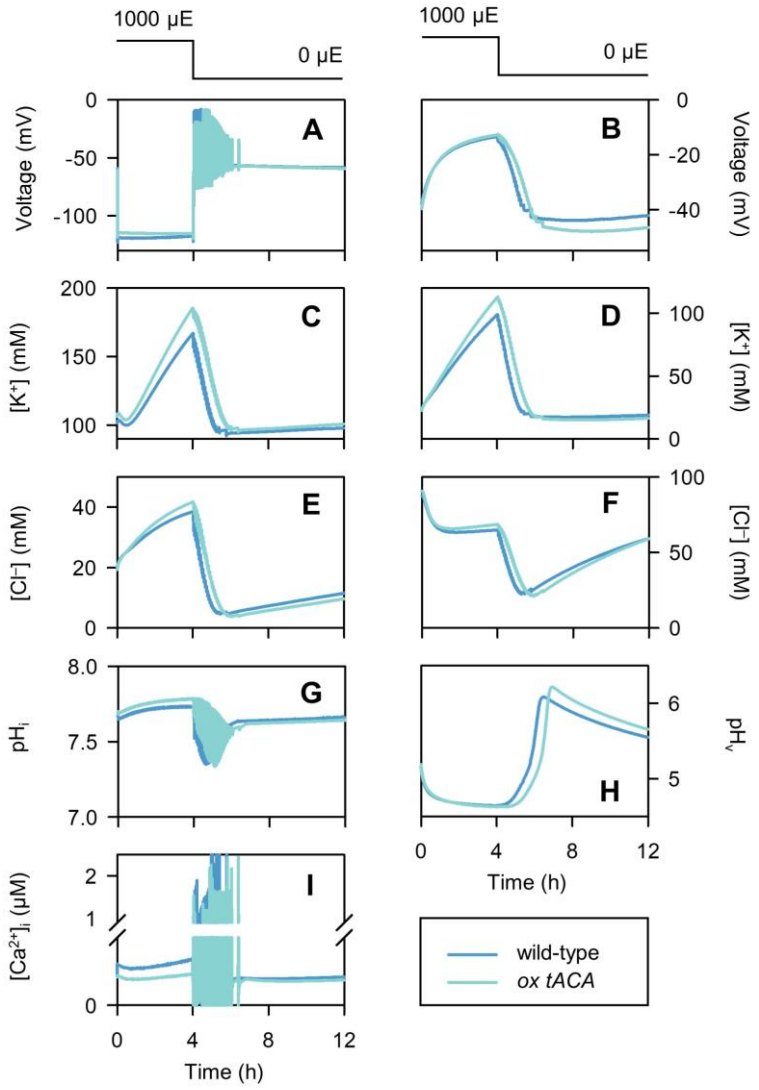

869

870 **Figure 3. Selected microscopic outputs derived from OnGuard modelling of wild-**
871 **type and *ox tACA* plants.**

872 (**A-I**) plasma membrane (**A**) and tonoplast (**B**) voltage, K^+ concentration in cytosol (**C**)
873 and vacuole (**D**), Cl^- concentration in cytosol (**E**) and vacuole (**F**), pH in cytosol (**G**)
874 and vacuole (**H**), and (**I**) cytosolic free Ca^{2+} concentration, $[Ca^{2+}]_i$.

875

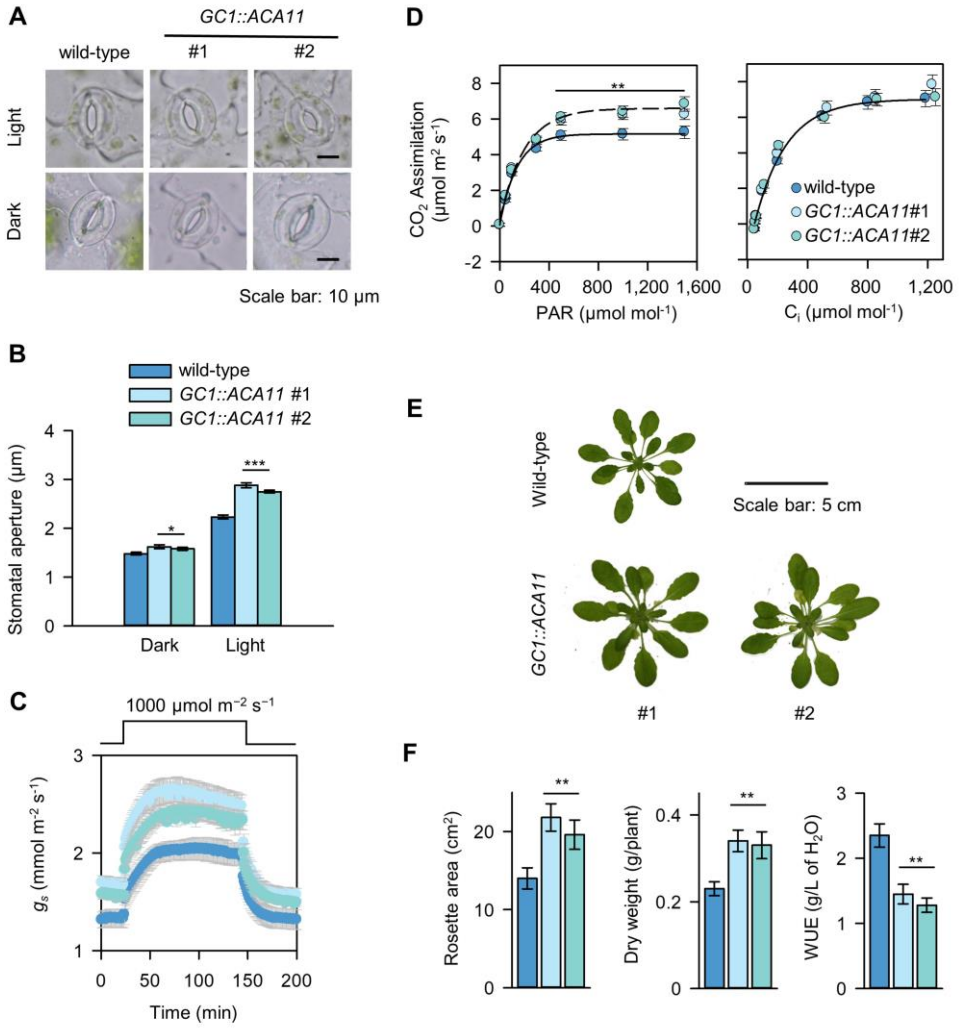

876

877 **Figure 4. *GC1::ACA11* plants exhibit larger stomatal aperture and improved**
878 **growth.**

879 (**A**) Representative stomata of wild-type and *GC1::ACA11* lines under light and dark.
880 (**B**) Stomatal aperture of wild-type and *GC1::ACA11* lines under light and dark. Data
881 are means ± SE (n = 30). Asterisks indicate statistically significant differences
882 compared with wild-type (* $p \leq 0.05$, *** $p \leq 0.001$). (**C**) Stomatal conductance (g_s)
883 recorded from intact plants of *GC1::AHA2* lines (n = 5) and wild-type (n = 5) on the
884 indicated time period. (**D**) Light response and CO_2 response curves of wild-type and
885 *GC1::ACA11* lines. Data are means ± SE (n = 5). Asterisks indicate statistically

886 significant differences compared with wild-type (** $p \leq 0.01$). (**E**) Representative wild-
887 type and *GC1::ACA11* lines grow under normal condition. (**F**) The rosette area, dry
888 weight and WUE of *GC1::AHA2* lines ($n = 5$) and wild-type ($n = 5$). Asterisks indicate
889 statistically significant differences compared with wild-type (** $p \leq 0.01$).
890

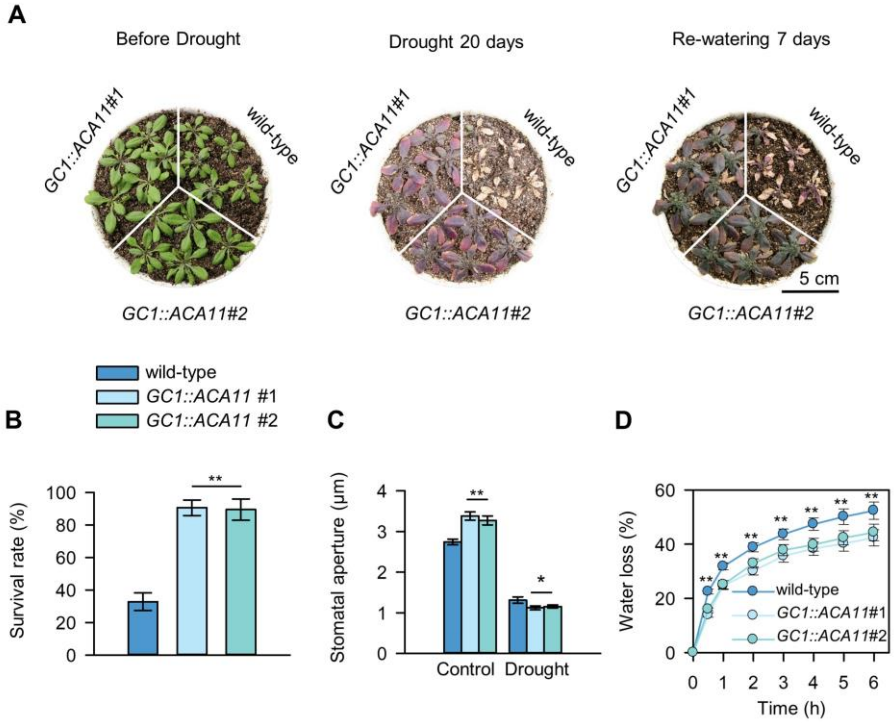

891

892 **Figure 5. *GC1::ACA11* plants exhibit improved drought tolerance.**

893 (**A**) Comparison of wild-type and *GC1::ACA11* lines under control, drought stress and
894 re-watering conditions . (**B**) Survival rate of wild-type and *GC1::ACA11* lines after re-
895 watering. Data are means ± SE (n = 10). Asterisks indicate statistically significant
896 differences compared with wild-type. (**C**) The stomatal aperture of wild-type and
897 *GC1::ACA11* lines under control and drought stress. Data are means ± SE (n = 60).
898 Asterisks indicate statistically significant differences compared with wild-type (* $p \leq$
899 0.05, ** $p \leq 0.01$). (**D**) The water loss from intact leaves of wild-type (n = 5) and
900 *GC1::ACA11* lines (n = 5). Asterisks indicate statistically significant differences
901 compared with wild-type (** $p \leq 0.01$).

902

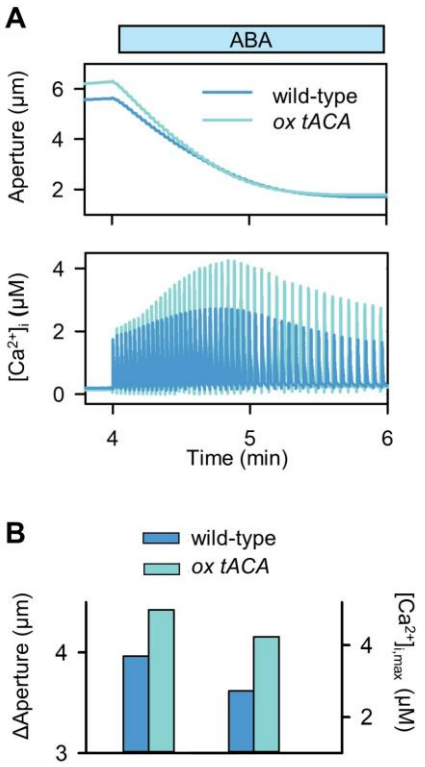

903

904 **Figure 6. OnGuard modelling and experimental validate of wild-type and**
905 ***GC1::ACA11* plants in response to ABA.**

906 (**A**) Simulating the changes in stomatal aperture and $[Ca^{2+}]_i$ in response to ABA. (**B**)
907 The changes in stomatal aperture and the maximum $[Ca^{2+}]_i$ derived from OnGuard
908 predictions.

909

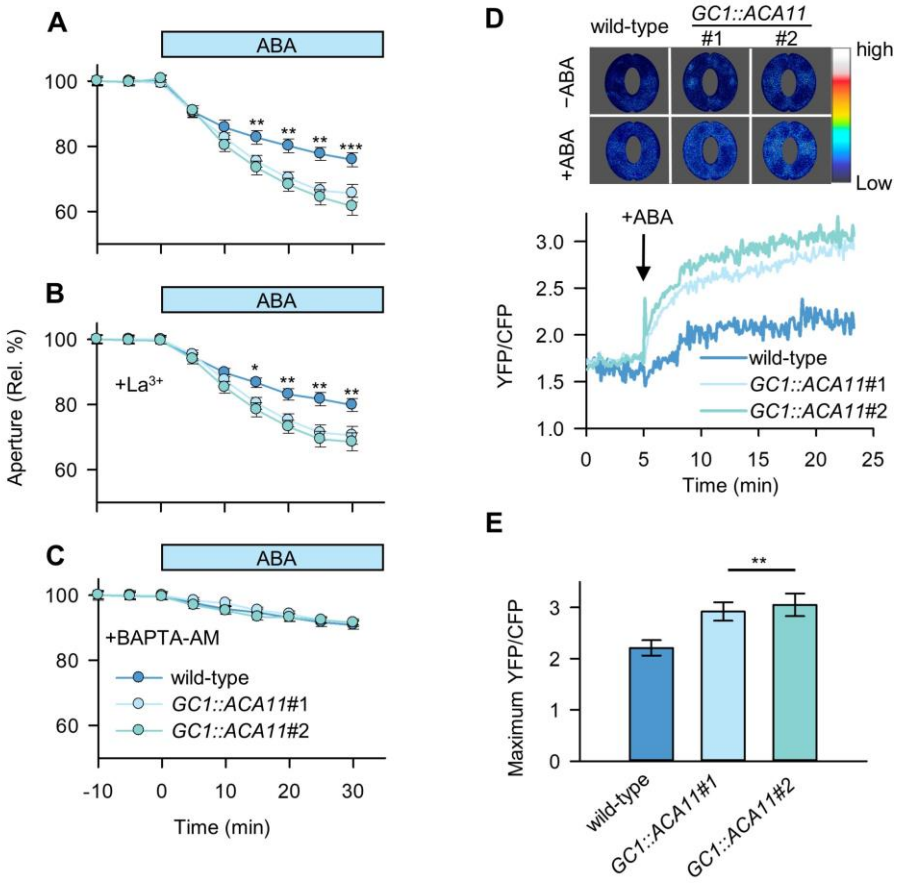

910

911 **Figure 7**. **Experimental validate of wild-type and *GC1::ACA11* plants in response**
912 **to ABA.**

913 **(A)** Experimental results of relative stomatal aperture changes in wild-type (n = 50) and
914 *GC1::ACA11* plants (n = 50) in response to ABA. **(B)** Relative stomatal aperture
915 changes in wild-type (n = 50) and *GC1::ACA11* plants (n = 50) pre-incubated with 100
916 μM $LaCl_3$ in response to ABA. **(C)** Relative stomatal aperture changes in wild-type (n
917 = 50) and *GC1::ACA11* plants (n = 50) pre-incubated with 25 μM BAPTA-AM in
918 response to ABA. Asterisks indicate statistically significant differences compared with
919 wild-type (* $p \leq 0.05$, ** $p \leq 0.01$, *** $p \leq 0.001$). **(D)** Representative YFP/CFP
920 recorded images of wild-type and *GC1::ACA11* YC3.6 transgenic plants in response to
921 ABA. **(E)** The maximum YFP/CFP from wild-type (n = 10) and *GC1::ACA11* YC3.6
922 transgenic plants (n = 10). Asterisks indicate statistically significant differences
923 compared with wild-type (** $p \leq 0.01$).

924

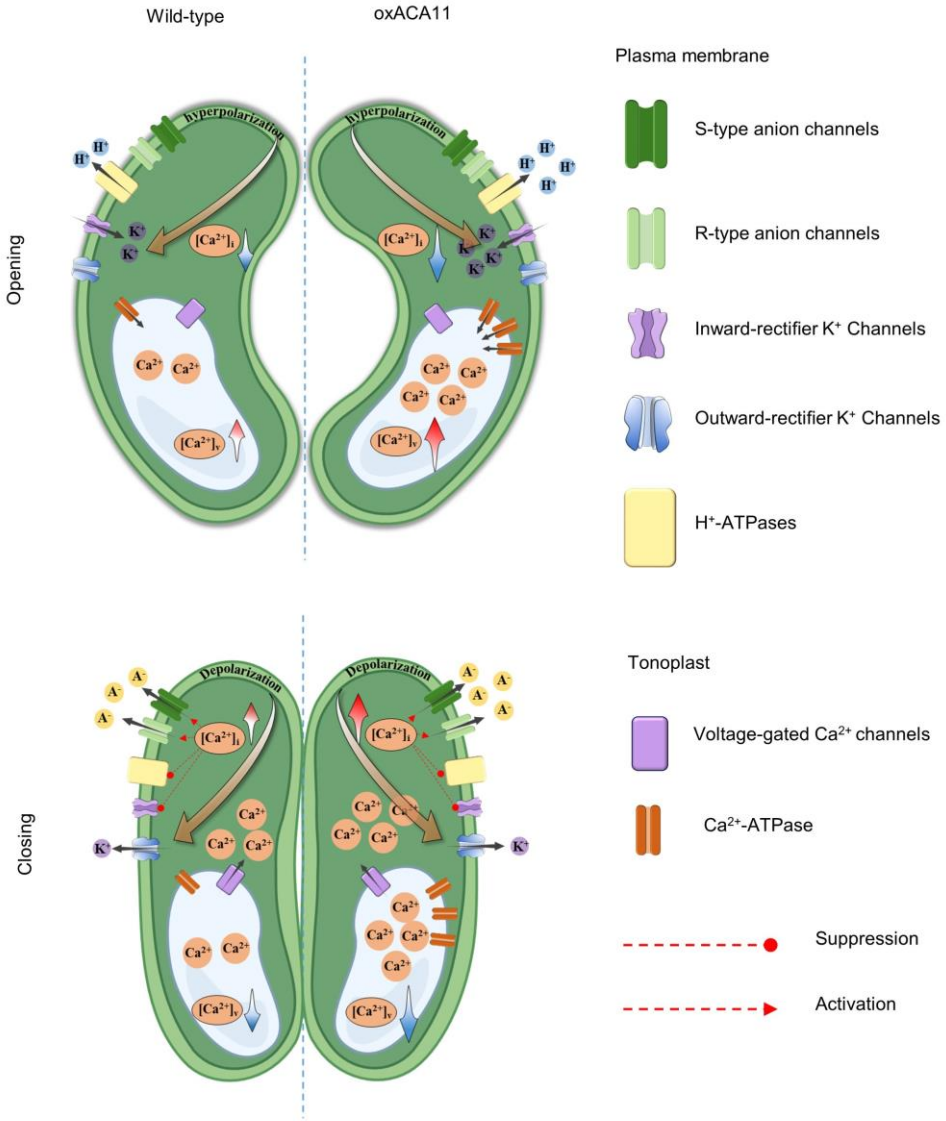

925

926 **Figure 8. Proposed working model of the role of overexpressing ACA11 on**
927 **stomatal movements.**

928 In the process of stomatal opening, overexpression of ACA11 leads to an excessive
929 accumulation of Ca^{2+} in the vacuole. This increased Ca^{2+} concentration in the vacuole
930 results in a reduction of $[Ca^{2+}]_i$. As a consequence, the reduced $[Ca^{2+}]_i$ enables the
931 uptake of osmotic solutes, which enhances stomatal opening. Conversely, during
932 stomatal closing, the large store of Ca^{2+} in the vacuole facilitated by overexpressed
933 ACA11 promotes an elevation of $[Ca^{2+}]_i$. This elevated $[Ca^{2+}]_i$ triggers the release of
934 osmotic solutes, ultimately leading to large stomatal closure.

935

AVAILABILITY OF MATERIALS

All pGC1-Dest vectors described in this article are available for academic and non-profit use on request from Michael Blatt (Michael.Blatt@glasgow.ac.uk). All other data generated and analysed during this study are included in this published article and its supporting information files and are also available on reasonable request to the corresponding author.

Jinghan Su

Yizhou Wang